Next-Generation Custom-Fit Reusable Respiratory Protective Device with Continuous Fit Monitoring – Part I: Custom-Fit Design

Sungmee Park[1], Yuanqing Tian[2], Michael Bergman[3], Jonisha Pollard[3], Ziqing Zhuang[3], and Sundaresan Jayaraman[1]*

1. Georgia Institute of Technology, School of Materials Science and Engineering, Atlanta GA USA

2. Georgia Institute of Technology, School of Industrial Design, Atlanta GA USA

3. National Institute for Occupational Safety and Health, Pittsburgh PA USA

* Corresponding author email: sundaresan.jayaraman@gatech.edu

ABSTRACT

Filtering facepiece respirators (FFRs) are manufactured in discrete sizes, with some models being limited in relation to accommodating the fit of some sex and race combinations. This study presents the development of a custom-fit respiratory protective device (RPD) which conforms to a user's facial features and flexes and moves with facial movements during use. Our design also integrates a pressure-sensing network, which continuously monitors fit and will alert the user when the fit is compromised.

In this three-part series of papers, we design, develop, and successfully demonstrate the realization of a custom-fit reusable RPD comprising the technology building blocks of a base frame, a covering piece, interlocking screw sets, a fastening hub, and a continuous fit monitoring system. By facilitating the customization of the RPD – ensuring the right fit and choice of filter with the desired degree of filtration – this device may have high acceptability by the public, including children, for whom RPD options are currently limited.

In this first paper, we develop the methodology, including the algorithms, for automating the design and production of custom-fit RPDs from digitally scanned facial profiles of individuals. We propose a taxonomy of anthropometric facial landmarks for customizing an RPD for an individual. We demonstrate the successful application of the taxonomy by creating digital prototypes of custom-fit RPDs for three individuals with different facial profiles.

Keywords: Custom-fit respiratory protective device; anthropometric features; facial landmark taxonomy; 3D digital scanning; protection; comfort; additive manufacturing.

INTRODUCTION

Protection of healthcare workers in the event of an influenza pandemic is a national imperative and personal protective equipment (PPE) is at the front line of defense. The COVID-19 pandemic has reinforced the importance of PPE, especially N95® filtering facepiece respirators (FFRs) approved by the National Institute for Occupational Safety and Health (NIOSH), for healthcare workers (Institute of Medicine, 2008; Institute of Medicine, 2006; National Academies of Sciences, Engineering, and Medicine, 2019). More recently, a National Academies of Sciences, Engineering, and Medicine (2022) study developed frameworks for providing respiratory protection against inhalation hazards for the public and workers outside of workplace respiratory protection programs. The need to make respiratory protective devices available and accessible to the public was one of the study's recommendations. The present research lays the foundation for realizing such a device for the public including children.

Respiratory Protection: A Systems Perspective

Figure 1 shows a systems perspective of respiratory protection. As demonstrated, the effectiveness of protection offered by a respiratory protective device (RPD) against an inhalation hazard for a user is a function of the *efficacy* of the device, *compliance* with its use, and a *commitment* by manufacturers to produce the needed products, including pathways or means to make it available for the user to access the right type of device at the right time.

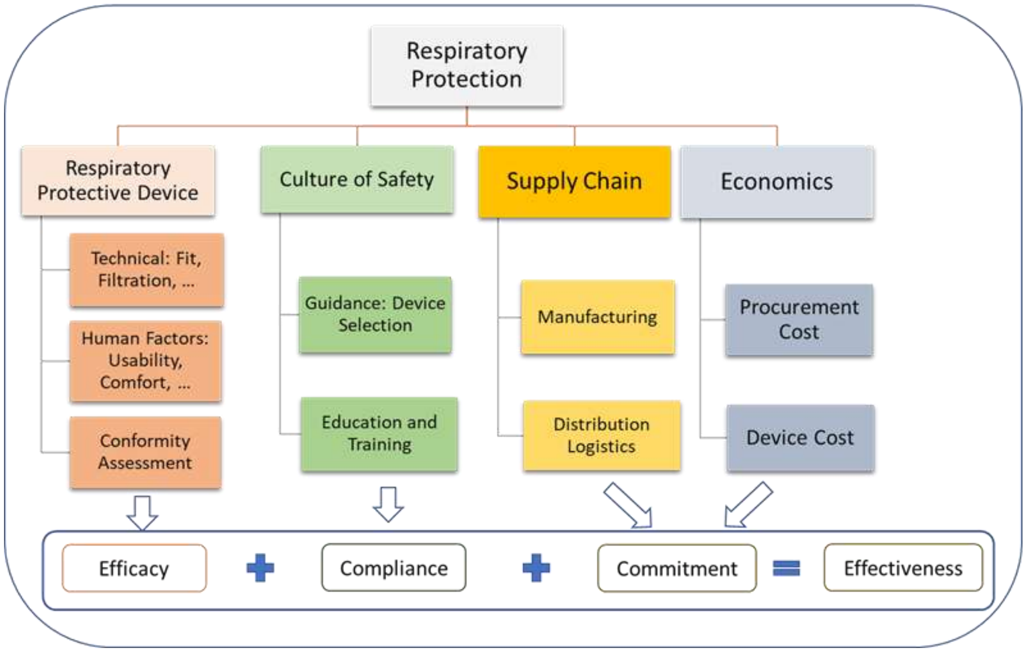

Figure 1. Respiratory protection: A systems perspective.

The efficacy of an RPD, such as an N95 FFR, is determined by technical factors such as fit and filtration efficiency, human factors such as usability and comfort, and conformity to performance standards. The overarching culture of safety, which encompasses guidelines for selecting the right device, education, and training, is critical for compliance with the use of the device. In the U.S., fit testing is required for tight-fitting respirators, including FFRs, under Occupational Safety and Health Administration regulations (OSHA, 2019). Fit testing is both time-consuming and expensive to administer. Manufacturing commitment is determined by the existence of a robust supply chain with a responsive manufacturing base and distribution system that ensures the availability of the device in a manner that is cost-effective for the end user. The critical shortages of FFRs experienced at the onset of the COVID-19 pandemic reinforced the need for a systems perspective to protect healthcare professionals and the public successfully (Contrera, 2020).

Objective of the study

The primary objective of the research reported in this three-part series of papers is to design, develop, and test a custom-fit reusable RPD with continuous fit monitoring. In Part I, we lay the foundation for the automation of the processes from facial scanning to prototype testing by developing algorithms to identify the required landmarks for any facial profile and using them to produce a custom-fit RPD. The developed RPD will facilitate easy replacement of the filter and decontamination of the frame after use. In Part II, we design and incorporate a continuous fit monitoring system in the RPD designed in Part I to enhance its role in protecting users from inhalation hazards in an effective manner during its use. In Part III, we transform the digital prototypes of the custom-fit RPD presented in Parts I and II to physical prototypes through 3D printing (additive manufacturing) using silicone-based elastomers. We test and quantify the responsiveness of the RPD with continuous fit monitoring to changes in facial profile from neutral expression, to talking, to smiling, to yawning.

Here we focus on the design of the RPD, which is critical because it affects the other facets of the system shown in Figure 1. Specifically, it influences all the outcomes – i.e., efficacy, compliance with use, and commitment to produce and make it accessible – which ultimately determine the effectiveness of respiratory protection both during normal times and during emergencies caused by, for example, respiratory disease outbreaks and wildfires. In the absence of manufacturing surge capability to produce different types and quantities of RPDs rapidly, the current practice for emergency preparedness typically involves stockpiling multiple models of disposable FFRs in an attempt to accommodate a range of facial features. The stockpile also includes elastomeric half-mask respirators (EHMRs), which are reusable. However, there is no guarantee that the correct model will be available in the stockpile and accessible at the point where and when it is needed during an emergency. Therefore, the design and realization of a reusable RPD that is customized to the user's facial profile and maintains its fit during use is important, and is the focus of this research. For the purpose of this series of papers, an RPD is defined as any device designed to protect the wearer's respiratory tract against the inhalation of a hazardous atmosphere that claims to meet a recognized voluntary consensus standard (e.g., ASTM, ANSI) or national regulation/standard (e.g., 42 CFR Part 84) that includes an assessment of minimum filtration efficiency level. These RPDs would also provide some level of source control that would additionally be improved when custom-fit. According to the CDC's NIOSH Science blog, "source control refers to the use of masks to cover a person's mouth and nose and to help reduce the spread of large respiratory droplets to others when the person talks, sneezes, or coughs" (CDC, 2020).

Facial features and anthropometry

The shape of the human face is complex and diverse due to a multitude of reasons including sex, race, and demographics (Chopra *et al.*, 2021). Zhuang and Bradtmiller (2005) surveyed the head-and-face anthropometrical measurements among U.S. respirator users, including over 3,997 subjects, and covering males and females from three major ethnicities in the U.S. (Caucasian, African American, and Hispanic) and the majority of age ranges (from 18 to 66). The captured head-and-face size distribution among the U.S. population includes 26 landmarks and 21 dimensions. These landmarks and dimensions cover both face size evaluation and head size. These have been valuable for manufacturing FFRs since they can help categorize size ranges and aid in fitting them to users. In their study on fit panels, Zhuang *et al.* (2008) quantitatively analyzed respirator size fit for different users in terms of pre-defined size ranges. They found outliers and improper fit in small and large size ranges. Lui *et al.* (2015) studied the variations in head-and-face shape among Chinese civilian workers to address the challenge associated with the use of Western anthropometric data to design RPDs for Chinese workers. They used principal component analysis to analyze the variability in head-and-face shape of 3D images of 350 participants, who were selected from the 3000 participants in the 2006 Chinese Anthropometric Survey. They found that more than 90% of the variability among head-and-face shapes was accounted for with 26 principal components.

Oestenstad *et al.* (2007) examined the relationship between facial dimensions and respirator fit considering the effect of gender and respirator brand. They found that bigonial breadth and menton-nasion length were significantly associated with respirator fit in five of the six models they studied, and biectoorbitale breadth, bizygomatic breadth, and lip width were significantly associated with respirator fit in four of the six models. They concluded that all these facial dimensions should be considered in the design of FFRs and that face length and lip width alone may not be appropriate in defining test groups whose fit is intended to be representative of worker populations. Kim *et al.* (2003) collected facial anthropometric data for Koreans to identify facial dimensions that would be appropriate for that population since FFR fit and performance analyses were typically done for Whites or male subjects. They found that Korean males and females had different facial dimensions compared to those of white males and females. They found that the facial dimensions that were significant in influencing FFR fit were different from the traditional facial dimensions of face length and lip width. They recommended that those distinct facial characteristics must be considered in the design of FFRs for the Korean population.

Lin and Chen (2017) investigated the effect of FFR style on the fit experience of an Asian population. They used three shapes of FFR models: Cup, Fold, and Liner FFR models, which have distinct edge contours. The Cup FFR was a cup-shaped FFR, the Fold model had a three-panel flat fold, and the Liner FFR was similar to a Cup FFR but was lined with an elastomeric faceseal band around the rim inside the facepiece. Based on the fit panel test and data analysis, they concluded that the Fold model fit significantly better than the other two models for medium and large Asian facial size groups. Furthermore, today's practice of producing FFRs in a few sizes limits users' options, which is further constrained by what is made available to them at the point of use, and leads to challenges with fit and comfort, thereby potentially compromising the degree of protection for the diverse population of users.

Importance of Fit and Continuous Fit Monitoring in Respiratory Protection

The pressure exerted by an RPD, e.g., an FFR, on the face at the interface affects both the comfort of the wearer and the leakage at the interface, which is the faceseal. Roberge *et al.* (2012) studied the importance of tethering devices that hold an FFR on the face during repeated doffing and donning. They found "a progressive decline in the loads generated by the top and bottom tethering devices of the three models of N95 FFR tested over the course of multiple simulated donning, doffing, and wear periods in a 2.5-hr span." This change in load (and hence, pressure) on the faceseal could alter the "fit" of the RPD, leading to leakages and thereby compromising the degree of rated protection from the device. Studies have also shown that the pressure exerted by the tethering devices is inversely proportional to the contact surface areas of the faceseal (Yang *et al.*, 2009).

Grinshpun *et al.*, identified two penetration pathways into an RPD that affected its protection level: (1) through the faceseal leakage, and the (2) filter medium (Grinshpun *et al.*, 2009). They assessed the contributions of these two pathways for particles in the size range of 0.03 to 1 μm under actual breathing conditions. They found that most of the penetrated particles entered through the faceseal and concluded, "the priority in respirator/mask development should be shifted from improving the efficiency of the filter medium to establishing a better fit that would eliminate or minimize faceseal leakage." Likewise, a better fitting RPD that eliminates or minimizes faceseal leakage will also eliminate or minimize the transfer of particles from the user to the environment and thereby enhance its source control function.

The pressure exerted by the RPD on the faceseal influences the comfort of the user and tolerability of the RPD and was reported as one of the reasons for the discontinuation of the use of an RPD in a health care setting (Radonovich *et al.*, 2009). Currently, for RPDs, there is no routine "quantitative" metric or indicator that users can rely upon to know that the device has been donned correctly to ensure proper fit so that they will be protected while also being comfortable. That "sense of security" for healthcare professionals using RPDs in the field is a critical factor in enabling them to perform at their best under trying circumstances (e.g., during COVID-19) without being afraid of compromising their personal safety. Zhuang *et al.* (2017) tested 101 different FFRs using panels of 25 subjects for each model. Only 32% of the devices achieved acceptable fit in at least one of three donnings for greater than 75% of participants. Therefore, continuous monitoring of pressure at the faceseal of an RPD, which will serve as a reliable indicator for fit, is critical for ensuring both the comfort and effectiveness of the device during use. This pressure distribution changes during RPD use, i.e., when the user is talking, smiling, or yawning. If the RPD is responsive to changes in the facial profile and maintains contact with the face during those changes, there will be no faceseal leakage. Thus, by monitoring the pressure distribution continuously, it is possible to detect changes in fit that could lead to faceseal leakage and alert the user to adjust the RPD in real-time to ensure the degree of protection for which the RPD is designed.

The ability to "calibrate" the fit with the measured pressure at the faceseal is also likely to lead to increased compliance with the correct use of the device. During the initial fit test with such a device, quantitative baseline parameters could be established. Any change in these values during use that compromises the fit of the RPD would trigger appropriate alerts, prompting the user to adjust the device to avoid potential leakage at the faceseal. This feature will overcome one of the key challenges with the "user seal check," which has been shown to not be a reliable substitute for quantitative fit testing when using FFRs (Lam *et al.*, 2011).

The fit of the RPD, especially over long durations of wear, is another important factor. A tight-fitting respirator used continuously over long durations may cause skin irritation, injury, and pain (Stokowski, 2020; Lam *et al.*, 2020). Therefore, continuous monitoring of faceseal pressure can also provide information to the user to prevent pressure injuries associated with long-term use of respirators (NPIAP, 2020). In fact, the cost of treating pressure injuries is estimated to be 2.5 times the cost of preventing them (Oot-Giromini *et al.*, 1989). Therefore, there is a critical need for fit monitoring data that can be harnessed to facilitate "evidence-based" decision-making on the safe use of RPDs over extended periods.

Research on Optimally-fitted FFRs

Cai *et al.* (2018) provide a comprehensive assessment of previous research on designing optimally-fitted FFRs including the use of 3D scanning and rapid prototyping. In their own work, they fabricated faceseal prototypes using Acrylonitrile Butadiene Styrene (ABS) plastic on an FDM (fused deposition modeling) printer. They developed a force sensor system that was inserted between the FFR and the headform to measure the pressure at the faceseal. However, due to the limitations of the force sensor system, they could measure the contact pressure at only a single point at a time. Consequently, they could not concurrently monitor the fit throughout the faceseal in real time, which is critical to always ensure the desired degree of protection to the user. Jayaraman and Park (2020) proposed the concept of scanning an individual's face to create a custom-fit RPD frame with a replaceable filter of desired protection level (e.g., filtration level of an N95FFR). After use, the filter would be discarded and the RPD frame decontaminated, rendering it ready for use with a new filter.

Need for the research and objectives

The complexity of the diverse human face shapes requires an enhanced and more flexible method to design an RPD customized to a user's facial features. The RPD should also facilitate the use of filters with desired filtration efficiencies depending on the degree of protection needed against specific inhalation hazards. The RPD should be reusable to address the supply chain shortages witnessed during the onset of the COVID-19 pandemic. Therefore, the design should facilitate the replacement of the filter and easy decontamination of the RPD frame after each use. Further, the ability to monitor the fit continuously, and alert the user as needed, is valuable for providing the sense of security needed by users working in high-risk and high-stress environments, such as hospitals with COVID-19 patients. The published research has not revealed a comprehensive solution. Therefore, harnessing advanced technologies, including 3D scanning and additive manufacturing, for the development of a reusable RPD has the potential to enhance the fit experience and effectively address the long-standing issues with today's mass-produced FFRs.

METHODS

This section describes an iterative design and development cycle comprising 3D scanning of a facial profile through the realization of a digital prototype of a custom-fit RPD with continuous fit monitoring.

Selection of Anthropometric Facial Landmarks and Dimensions

The first step in designing a custom-fit RPD is to understand the human facial anthropometric data including anatomic landmarks, dimensions, and contours that define an individual's facial profile. These anthropometric characteristics will be used as "references" for customizing the RPD for any facial profile. The key challenge lies in identifying the right set of these anthropometric facial landmarks. We used the NIOSH study identifying 26 pre-defined landmarks and 21 facial dimensions as the starting point (Zhuang & Bradtmiller, 2005). We chose 18 of the 26 facial landmarks that focused on the lower face (below the nasal root points since the proposed device is analogous to a half-facepiece respirator). Figure 2 shows these landmarks.

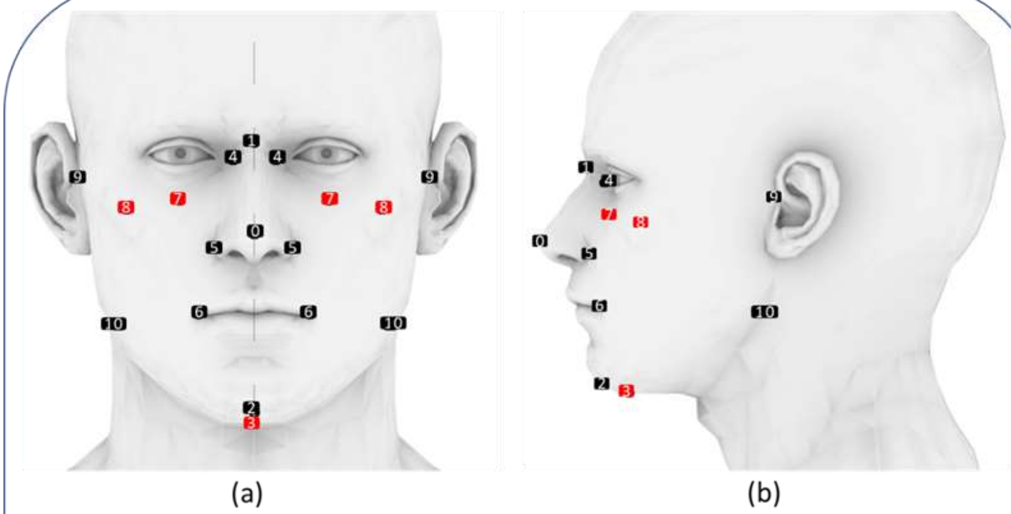

Pronasale (0)	Cheilion (6, 6)
Sellion (1)	Infraorbitale (7, 7)
Chin (2)	Zygomatics (8, 8)
Menton (3)	Tragions (9, 9)
Nasal Roots (4, 4)	Gonions (10, 10)
Alares (5, 5)	

18 Facial Landmarks

- Black: Guiding Landmarks
- Red: Physical Guiding Landmarks on RPD Contour

Figure 2. Facial landmarks for customizing RPD for facial profile. (a) Front view (b) Side view.

Among these selected landmarks, some are not directly relevant to the purpose of measuring either the face size or the base frame shape, but serve as reference points that can help us better position and orient the face images in horizontal and vertical planes. For example, the pupils, pronasale, chellions, and tragions can assist with balancing the symmetry for the facial image. The black landmarks in the figure aid in positioning, orienting, centralizing, and symmetrizing the scan data and mappings. The red landmarks fall on the contour of the frame.

In addition to selecting the landmarks, we needed to identify the specific dimensions that must be measured to characterize the facial profile. We chose 15 facial dimensions, six of which are from the NIOSH study of 21 facial dimensions (Zhuang & Bradtmiller, 2005); the others were identified specifically for creating a customized RPD. Eleven of these dimensions are straight-cut distances from point to point. The remaining four dimensions are straight-cut vertical ratio measurements, which, similar to reference landmarks, are reference proportion lines for positioning and orienting. Figure 3 shows the chosen facial dimensions for the design.

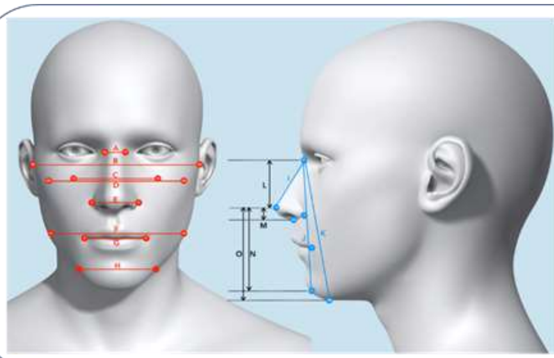

Nasal root breadth (A) *	Bitragion breadth (B)
Infraorbitale breadth (C)	Bizygomatic breadth (D) *
Nose breadth (E) *	Bigonial breadth (F) *
Lip length (G) *	Chin breath (H)
Nose length (I)	Sellion-chin length (J)
Menton-Sellion length (K) *	Pronasale-sellion vertical distance (L)
Pronasale-subnasale vertical distance (M)	Pronasale-chin vertical distance (N)
Pronasale-menton vertical distance (O)	

* Denotes one of NIOSH's 21 Dimensions

Figure 3. The chosen facial dimensions.

3D Scanning and Customized Frame Contour Development

For developing the customized RPD, we propose a design framework termed "3D to 2D to 3D," which spans the continuum from 3D image scanning of the facial profile to realizing the 3D-printed customized frame. It involves transformation of scanned 3D facial images into 2D frames followed by projecting these back to 3D structures for producing the physical frames.

We recruited three participants (2 females and 1 male) with different facial profiles for participation in the research. We used the 3dMD System (Temporal 3dMDface.t System, Atlanta, Georgia, USA) to scan the facial profiles (3dMD, 2020). The 3dMD face scanner captures the three-dimensional face image from ear to ear. The system is not designed to automatically recognize the facial anthropometrical or anatomical landmarks. Therefore, before scanning, we used a red lip-liner to mark the facial landmarks physically. We asked participants to look straight ahead and relax their facial expressions while the 3D cameras recorded a 10-second footage with over 100 scan frames. The exported files for each participant contain all the frames in OBJ file format with colored textures; we can see the landmarks clearly on the faces. One benefit of the 10-second footage and multiple frames is that we could examine all the images and select images that had no blurs or noise due to the inevitable shaking, swinging, or blinking that occurs during scanning.

We used 3dMD Vultus, the software that comes with the 3dMDface™ System, to process the scanned image. We re-marked the landmarks virtually and measured the dimensions. We applied different tools (plane cut, mask, and refinement) to cut off the unwanted debris and fragments (e.g., hair texture) to focus on the front face area. The core task was to use the measurement and analysis tools to digitize the landmarks and dimensions. We created analysis scripts for the landmarks and dimensions in order to analyze the scanned profiles of the subjects. With the available landmark and analysis (dimension) scripts, we overlaid the points onto the physical landmarks and placed marks onto the non-contactable landmarks (e.g., pupils). In the built-in world coordinate system, each landmark has a coordinate (x, y, z) and the origin (0, 0, 0) can be placed in any desired location. We settled on the pronasale point – the center reference point on the face – as the origin (0, 0, 0); the other landmarks were accordingly updated to their new coordinates. This helped us understand the overall relationship between all the landmarks easily and quickly. Subsequently, the analysis script automatically generates a report file for all the dimensions measurements we need. Figure 4 shows the scanned images of one of the participants in 3dMD's Vultus program.

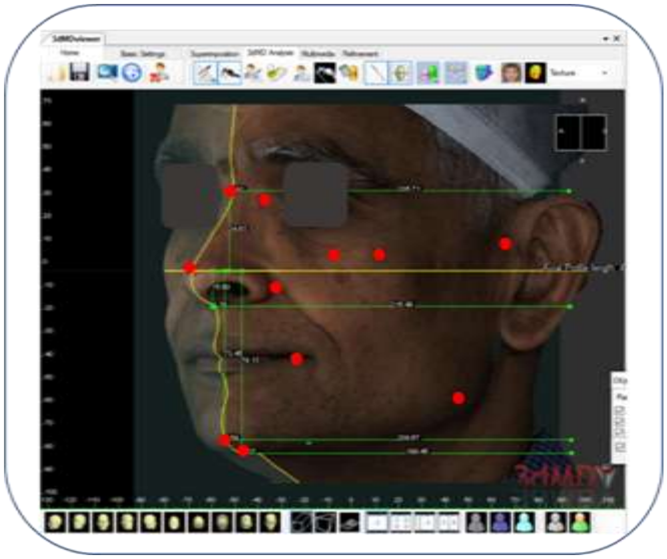

Figure 4. Scanned images of a subject in 3dMD Vultus software.

Defining a Taxonomy of Landmarks

We imported the textured scanned data into Rhino® CAD software to construct the 3D model of the RPD frame. With the pronasale point as the origin of the coordinate system, we mapped out the other landmarks by placing the exact three-dimensional coordinates in the Rhino software coordinate system. The first step in the "3D to 2D to 3D" design methodology is "3D to 2D," which refers to a geometrical projection of all the three-dimensional landmarks onto a two-dimensional plane that is parallel to the coronal plane. Thus, we acquired a 2D mapping that deploys all the landmarks with their relationships on lateral (horizontal or Y-axis) and medial (vertical or Z-axis) directions.

The next step is to augment the chosen facial landmarks in Figure 3 with landmarks on the side of the face and the jaw area for drawing a smooth contour of the RPD frame. We followed the "3D to 2D to 3D" design framework to project all the pre-defined physical landmarks onto both front view 2D plane and right-side view 2D plane. This provides a better understanding of the numerical and geometrical relationships of the landmarks and facilitates the identification of new ones for drawing the smooth contour of the RPD frame. This initial set of landmarks, which we term "Defined Landmarks," is not adequate for drawing a smooth contour of the entire RPD frame. Therefore, we developed algorithms to identify new landmarks on the front view 2D mapping. These new landmarks are "derived" based on the Defined Landmarks and are named "Derived Landmarks."

Derived Landmark D1: One of the challenges during the use of FFRs is the interference of the top edge of the device with users wearing eyeglasses. Consequently, the use of sellion or nasal root as one of the landmarks for defining the contour of the RPD frame would not be appropriate as this contour could cause interference. To identify the correct location for the landmark for the top edge of the frame, we measured the straight-cut distance from the sellion to pronasale (termed "nose height") for the three subjects. The three subjects then wore two different FFR models (a cup-shaped model and a duckbill-shaped model) to determine where the top edge of the FFRs fell on the sellion-pronasale line. The average point of the top edge of the FFR for the three subjects was at 57% from the pronasale on the sellion-pronasale line. To accommodate the sensor network for continuous fit monitoring, we allocated a 10-mm width for the RPD frame. Therefore, we chose the location at one-half nose height as the inner edge of the frame. This means the midpoint of the sellion-pronasale line must be offset upward by 10 mm to locate the top vertex of the outer frame edge. Figure 5 shows the steps for arriving at D1, the top edge point for the contour of the frame. As seen in the figure, the algorithm utilizes the Defined Landmarks of pronasale and sellion as the foundation to identify D1, the Derived Landmark.

Derived Pair of Landmarks D2: To ensure that the frame fits well on the side of the face to prevent leakage, it is necessary to have a smooth contour of the frame near the jaw and the sides of the face. Therefore, we identified a pair of jaw side points (termed D2) between the chin point (2) and gonion (10) by following the steps shown in Figure 5.

Derived Pair of Landmarks D3: To ensure a proper fit and a smooth contour on the side of the face with a lot of soft tissue, it is important to have "intermediate" points between the Defined Landmarks. Therefore, we derived a pair of points on the left and right sides of the face (D3) as shown in Figure 5.

Developing the RPD Frame Contour: Using the Defined Landmarks and the Derived Landmarks, we draw the contour of the RPD frame by interpolating (curvilinear) between the points. We then project the contour on to the scan data with the face shape for each subject. The frame contours for the three subjects were smooth. However, the need to provide a 10-mm-wide surface to accommodate the sensor network in the frame for continuous fit monitoring made it harder to extend the frame near the menton (3) – one of the Defined Landmarks.

Derived Landmark D4: After a series of iterations, we arrived at a new Derived Landmark (D4) to replace the menton. Figure 5 shows the steps for deriving D4.

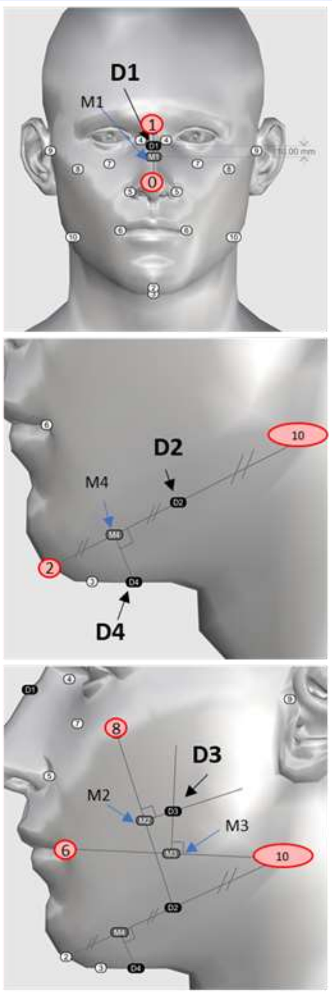

Algorithm for Location of D1 (Top Edge Point)

- Draw a straight line between Pronasale (0) and Sellion (1).
- Find the midpoint of line 0-1. Mark it M1.
- Offset the M1 point by 10mm upwards along the line 0-1 line; that point is D1.
- D1 is the top edge point for the contour of the RPD frame.

Algorithm for Location of D2 (Jaw Side Point)

- Draw a straight line between Chin (2) and Gonion (10).
- Find the midpoint of line 2-10. That is the D2 point. Similarly, locate the symmetrical point on the other side of the face.

Algorithm for Location of D4 (Jaw Point)

- Find the midpoint of line 2-D2. Mark it M4.
- Draw a perpendicular line from M4 until it intersects the jaw. That is D4.

Algorithm for Location of D3 (Face Side Point)

- Draw a straight line between Zygomatic (8) and D2. Find the midpoint of line 8-D2. Mark it M2.
- Draw a straight line between Chellion (6) and Gonion (10). Find the midpoint of line 6-10. Mark it M3.
- Draw perpendicular lines at M2 and M3.
- Find the intersection point of the two perpendicular lines. That is D3.

Figure 5. Identification of new landmarks: Algorithms for Top Edge Point (D1), Jaw Side Point (D2), Face Side Point (D3), and Jaw Point (D4).

Figure 6 shows the four Derived Landmarks on the digital scans of the three subjects by following the algorithms in Figure 5.

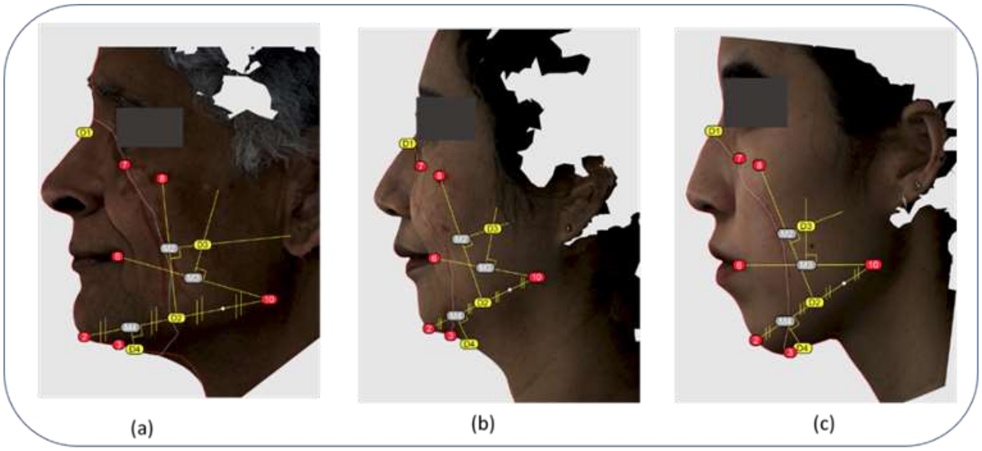

Figure 6. The four derived landmarks on the digital scans of the three subjects.

RESULTS AND DISCUSSION

We propose a taxonomy for the set of facial landmarks for developing the custom-fit RPD. As shown in Figure 7, the Defined Landmarks are those obtained from literature and which serve as the basis for identifying additional landmarks for developing the contour of the RPD frame. These Defined Landmarks are classified into Guiding Landmarks and Construction Landmarks. The Guiding Landmarks guide the design of the customized frame; for example, pronasale (0) serves as the origin (0, 0, 0) for the computations. The Construction Landmarks are used for constructing the final contour of the frame. The various intermediate landmarks that served to develop the final set of landmarks – based on geometrical relationships with the Defined Landmarks – are called Process Landmarks. These Process Landmarks are used to derive the Derived Landmarks. Thus, the customized frame contour is constructed using the Construction Landmarks and Derived Landmarks.

This taxonomy is expected to play a critical role in designing and developing a custom-fit RPD to fit any facial profile. The Derived Landmarks are based on well-defined steps (algorithms) drawing upon the Defined Landmarks as the foundation. Therefore, the process of creating a customized contour for any facial profile can be automated using the algorithms underlying the taxonomy shown in the figure. Figure 8 shows the locations of the various facial landmarks in the taxonomy.

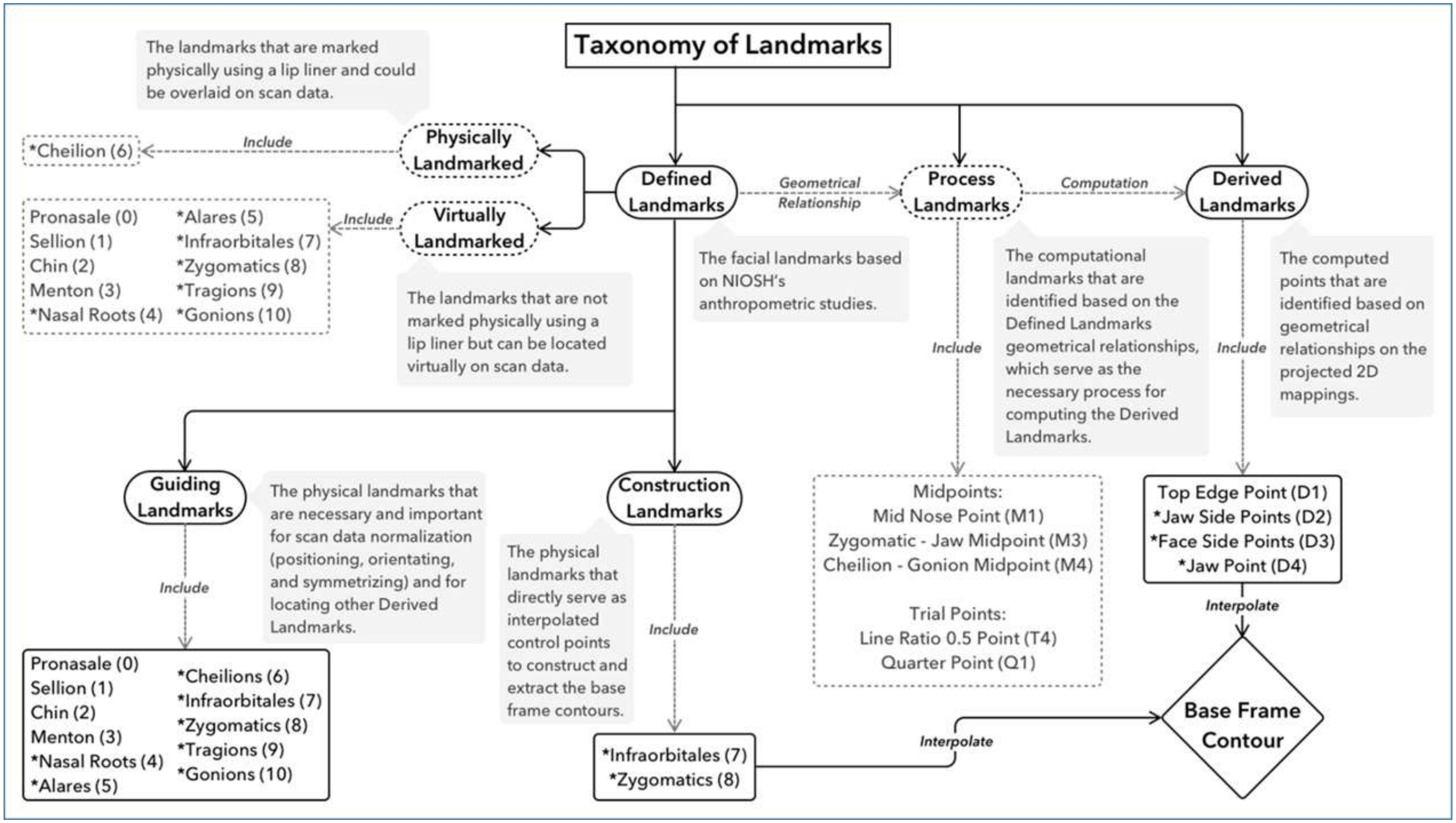

***** Indicates paired landmarks located symmetrically on both sides of the face.

Figure 7. The taxonomy of facial landmarks for creating a custom-fit RPD.

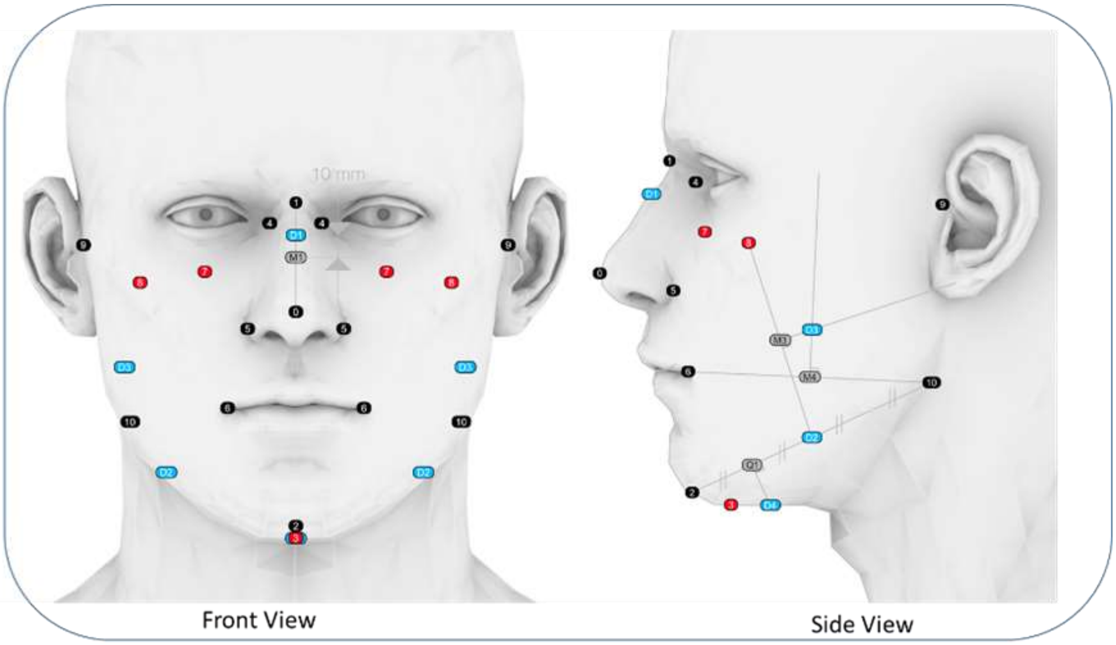

Figure 8. Landmarks in the developed taxonomy. Red: Construction Landmarks, Black: Guiding Landmarks, Blue: Derived Landmarks.

Figure 9 shows the realization of the RPD frame contour using the landmarks defined in the taxonomy. Beginning with the top edge point (D1) in the side view, we interpolate between the points infraorbitale (7), zygomatic (8), the face side point (D3), the jaw side point (D2), and the jaw point (D4). We then project this on to the face scan to obtain the frame contour that wraps onto the facial profile.

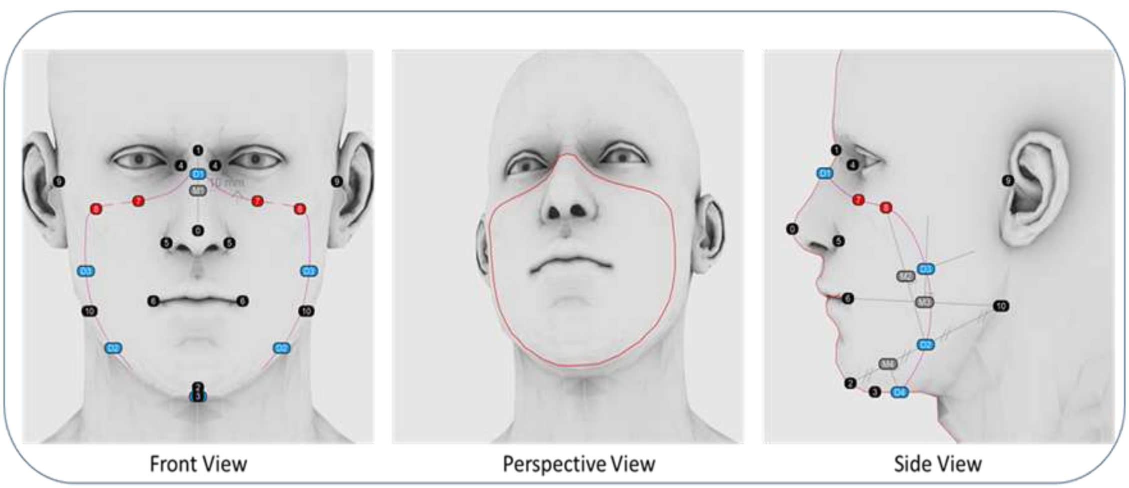

Figure 9. The realization of the custom-fit RPD frame using the landmarks in Figure 8.

Figure 10 shows the frame contours for the three subjects along with the landmarks used to create them.

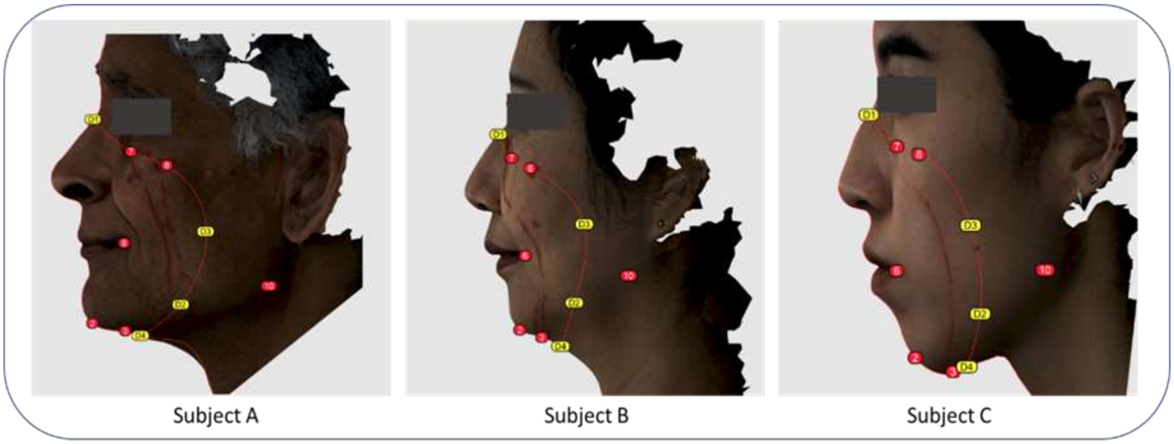

Figure 10. The RPD frame contour (Red) using the final set of landmarks.

Thus, the methodology utilizing the set of landmarks in Figure 7 led to the transformation of a scanned digital image of an individual's facial profile to a custom-fit digital prototype of the RPD frame. The realization of custom-fit digital frames for three subjects with different facial profiles demonstrates the applicability of the algorithm.

Limitations of the study

A key limitation of this study is that the final set of algorithms that led to the realization of customized RPDs was based on scanning the facial profiles of three individuals: two females and one male. Since the goal of the research was to develop a set of rules or algorithms that could be used to design and develop customized RPDs for any facial profile, the selection of individuals for scanning was not designed to be representative of a specific group or population. The three facial profiles were distinct and different. One of these facial profiles was used as a "base" to develop the algorithms and the other two facial profiles were used to test and refine the base algorithms through a series of iterations. This cycle was repeated multiple times and the generalizability of the algorithms improved with each cycle until the same algorithms could be used to create customized RPDs for the three individuals. In future research, the generalizability of the algorithm to address the needs of the diverse population should be explored. In the envisioned user-driven ecosystem, a distributed network of entities will carry out the various operations seamlessly from scanning the user at the site (e.g., health care facility), creating the customized digital frame, manufacturing the physical frame, integrating the fit monitoring system, testing, and delivering the customized RPD to the user. However, the realization of this ecosystem and its scalability for producing custom-fit RPDs, including the availability of compatible filters for use, have not been addressed in the study.

CONCLUSIONS

In this paper, we defined the methodology, including algorithms, for the design and development of a custom-fit respiratory protective device from digitally scanned facial profiles of individuals. We also proposed a taxonomy of facial landmarks for customizing the RPD for individuals and used it for developing the device. Finally, we created digital prototypes for three individuals with different facial profiles, thereby providing an initial demonstration of the robustness of the methodology and workflow and laying the foundation that could provide respiratory protection to the public including children, for whom RPDs are currently limited.

DISCLAIMER

The findings and conclusions in this report are those of the authors and do not necessarily represent the official position of the National Institute for Occupational Safety and Health, Centers for Disease Control and Prevention. Mention of any company or product does not constitute endorsement by the National Institute for Occupational Safety and Health, Centers for Disease Control and Prevention.

ATTRIBUTION

N95 is a certification mark of the U.S. Department of Health and Human Services (HHS) registered in the United States and several international jurisdictions.

ACKNOWLEDGEMENTS

Georgia Tech researchers acknowledge funding for this research from the U.S. Centers for Disease Control and Prevention under Broad Agency Announcement (75D301-20-R-68024) through contract number 75D30120C09567. The authors thank the anonymous reviewers for their helpful comments on the manuscript.

REFERENCES

Cai M., Li H., Shen S.,, Wang Y., Yang Q. (2018). Customized design and 3D printing of faceseal for an N95 filtering facepiece respirator. *Journal of Occupational and Environmental Hygiene*, 15:3, 226-234, https://doi.org/10.1080/15459624.2017.1411598.

Centers for Disease Control and Prevention (2020). Respiratory Protection vs. Source Control – What's the difference? https://blogs.cdc.gov/niosh-science-blog/2020/09/08/source-control/.

Chopra J., Abiakam N., Kim H. (2021). The influence of gender and ethnicity on facemasks and respiratory protective equipment fit: a systematic review and meta-analysis. *BMJ Global Health*, 6:e005537. doi:10.1136/bmjgh-2021-005537.

Contrera J. (2020). The N95 shortage America can't seem to fix, *The Washington Post*, September 21, 2020.

Grinshpun S.A., Haruta H., Eninger R.M., Reponen T., McKay R.T., Lee S.A. (2009). Performance of an N95 Filtering Facepiece Particulate Respirator and a Surgical Mask During Human Breathing: Two Pathways for Particle Penetration. *Journal of Occupational and Environmental Hygiene,* 6(10): 593-603.

Institute of Medicine (2006). *Reusability of Facemasks during an Influenza Pandemic: Facing the Flu*. The National Academies Press. https://doi.org/10.17226/11637.

Institute of Medicine (2008). *Preparing for an Influenza Pandemic: Personal Protective Equipment for Healthcare Workers*. The National Academies Press. https://doi.org/10.17226/11980.

Jayaraman S., Park S. (2020) Respiratory Protection Device. U.S. Patent 10,646,731, May 2020.

Kim H., Han D., Roh Y., Kim K., Park Y. (2003). Facial Anthropometric Dimensions of Koreans and Their Associations with Fit of Quarter-Mask Respirators, *Industrial Health* 41 8–18.

Lam S.C., Lee J.K.L., Yau S.Y., Charm C.Y.C. (2011). Sensitivity and specificity of the user-seal-check in determining the fit of N95 respirators, *Journal of Hospital Infection* 77 252-256. https://doi.org/10.1016/j.jhin.2010.09.034.

Lam U-N., Farah N.S., Siddik M., Yussof S.J.M., Ibrahim S. (2020) N95 respirator associated pressure ulcer amongst COVID- 19 health care workers, *Int Wound J*. October; 17(5): 1525–1527, doi: https://10.1111/iwj.13398.

Lin Y.C., Chen C.P. (2017). Characterization of small-to-medium head-and-face dimensions for developing respirator fit test panels and evaluating fit of filtering facepiece respirators with different faceseal design. *PLOS ONE*, 12(11), e0188638. https://doi.org/10.1371/journal.pone.0188638.

Liu Y., Xi P., Joseph M., Zhuang Z., Shu C., Jiang L., Bergman M., Chen W. (2015). Variations in Head-and-Face Shape of Chinese Civilian Workers, *Ann. Occup. Hyg*. 59: 7 932–944. doi:https://10.1093/annhyg/mev026.

National Academies of Sciences, Engineering, and Medicine. (2019) *Reusable Elastomeric Respirators in Health Care: Considerations for Routine and Surge Use*. Washington, DC: The National Academies Press. https://doi.org/10.17226/25275.

National Academies of Sciences, Engineering, and Medicine. (2022) *Frameworks for Protecting Workers and the Public from Inhalation Hazards*. Washington, DC: The National Academies Press. https://doi.org/10.17226/26372.

National Pressure Injury Advisory Panel. (2020) https://cdn.ymaws.com/npiap.com/resource/resmgr/position_statements/NPIAP_-_Mask_Injury_Infograp.pdf.

Oestenstad R.K., Elliott L.J., Beasley T.M. (2007). The Effect of Gender and Respirator Brand on the Association of Respirator Fit with Facial Dimensions, *Journal of Occupational and Environmental Hygiene*, 4:12, 923-930, DOI:10.1080/15459620701709619.

Oot-Giromini B., Bidwell F.C., Heller N.B. (1989). Pressure ulcer prevention versus treatment, comparative product cost study. *Decubitus*, 2(3), 52-4.

Occupational Safety and Health Administration (2019). § 1910.134 – Respiratory Protection. https://www.osha.gov/laws-regs/regulations/standardnumber/1910/1910.134.

Radonovich L.J., Cheng J., Shenal B.V,. Hodgson M., Bender B.S. (2009). Respirator Tolerance in Health Care Workers. *Journal of the American Medical Association.* 301(1):36–38. doi:10.1001/jama.2008.894.

Roberge R., Niezgoda G., Benson S. (2012). Analysis of Forces Generated by N95 Filtering Facepiece Respirator Tethering Devices: A Pilot Study, *Journal of Occupational and Environmental Hygiene,* 9 (8), pp. 527-533.

Stokowski L.A. (2020). A Step-by-Step Guide to Preventing PPE-Related Skin Damage. MedScape. Retrieved from https://www.medscape.com/viewarticle/929590.

Yang J., Dai J., Zhuang Z. (2009). Simulating the interaction between a respirator and a headform using LS-DYNA. *Computer-Aided Design Appl*. 6(4):539–551.

Zhuang Z., Bradtmiller B. (2005) A Head-and-Face Anthropometric Survey of U.S. Respirator Users. *Journal of Occupational and Environmental Hygiene*, Nov; 2 (11):567-76. DOI: https://10.1080/15459620500324727. PMID: 16223715.

Zhuang Z., Groce D., Ahlers H.W., Iskander W., Landsittel D., Guffey S., Benson S., Viscusi D., Shaffer R.E. (2008). Correlation between Respirator Fit and Respirator Fit Test Panel Cells by Respirator

Size. *Journal of Occupational and Environmental Hygiene*, 5(10), 617–628. https://doi.org/10.1080/15459620802293810.

Zhuang Z., Bergman M., Lei Z., Niezgoda G. Shaffer R. (2017). Recommended test methods and pass/fail criteria for a respirator fit capability test of half-mask air-purifying respirators. *Journal of Occupational and Environmental Hygiene*, 14, 473–481. https://doi.org/10.1080/15459624.2017.1296233.

3dMD. (2020) Retrieved from https://3dmd.com/products/.